

Recoil range study of complete and incomplete fusion of C with Au at 10 MeV/nucleon

D. J. Parker,^{(1)*} P. Vergani,⁽²⁾ E. Gadioli,⁽²⁾ J. J. Hogan,⁽³⁾ F. Vettore,⁽²⁾ E. Gadioli-Erba,⁽²⁾
E. Fabrici,⁽²⁾ and M. Galmarini⁽²⁾

⁽¹⁾*Nuclear Physics and Instrumentation Division, Harwell Laboratory, Oxfordshire OX11 0RA, United Kingdom*

⁽²⁾*Dipartimento di Fisica, Università di Milano, Milano, Italy*

and Istituto Nazionale di Fisica Nucleare, 20133 Milano, Italy

⁽³⁾*Department of Chemistry, McGill University, Montreal, Quebec, Canada H3A 2K6*

(Received 7 May 1991)

Cross sections and differential recoil range distributions have been measured for 22 spallation products formed in the interaction of 120 MeV ^{12}C with ^{197}Au . A Monte Carlo code has been produced that accounts for complete fusion as well as the transfer of α particles and ^8Be . The results of the calculation compare very well with the experimental data. Incomplete fusion is found to account for more than one-half of nonfission events, and preequilibrium emission of fast nucleons is essential to a full description of the reaction.

I. INTRODUCTION

At incident energies from the Coulomb barrier to about 10 MeV/nucleon, the system $^{12}\text{C} + ^{197}\text{Au}$ has been studied for more than 30 years. When the Berkeley HILAC opened, Gordon *et al.* [1] measured the fission cross section, angular distribution, and average kinetic energy of the fission fragments, assuming the reaction mechanism to be formation of a compound nucleus. They noted evidence, however, "for the emission of several particles" preceding the fission. Thomas *et al.* [2] then measured cross sections for astatine spallation products, again assuming compound nucleus formation followed by neutron evaporation, but noting the presence of competition from "charged particle evaporation." Twelve years later this work was greatly extended by Bimbot, Lefort, and Simon [3] and Stickler and Hofstetter [4]. In the first of many papers measuring fission fragment angular correlations, Sikkeland and Viola [5] noted that effectively almost all fissions occur following complete fusion.

The emission of α particles in the forward direction from these reactions had been known since the work of Britt and Quinon [6]. In 1972 Bimbot, Gardes, and Rivet [7] reported recoil measurements of spallation residues from the $^{12}\text{C} + ^{197}\text{Au}$ reaction at energies up to 90 MeV, which suggested that essentially all of these fast α particles were projectile fragments accompanying one or two alpha transfers from projectile to target, followed by spallation. Bimbot, Gardes, and Rivet measured excitation functions, angular distributions, and recoil ranges of seven Tl and Bi reaction products, attributable to transfer of an alpha particle and ^8Be , respectively, to the target, and were able to estimate the total cross section for each of the transfer processes as a function of energy. At 89 MeV they deduced a cross section for ^8Be transfer of about 130 mb; alpha transfer was clearly also significant, but their estimate of 85 mb was regarded as an upper limit.

This was perhaps the first clear evidence for the pro-

cess subsequently termed *incomplete fusion*, the nature of which was later established in particle-gamma coincidence studies of the $^{14}\text{N} + ^{159}\text{Tb}$ reaction by Inamura *et al.* [8]. It is now clear that incomplete fusion occurs for incident partial waves somewhat higher than those principally involved in complete fusion and can be thought of as a process in which the projectile breaks up near the surface of the target nucleus into two fragments, one of which escapes with relatively unchanged velocity, while the other fuses with the target to form an excited intermediate, which subsequently deexcites by particle evaporation in the usual way. However, systematic quantitative measurements of cross sections are rare.

Differential recoil studies are particularly attractive for studying these transfer processes. Even when a single reaction product is produced via several mechanisms, the linear momentum transfer is a signature of the interaction of projectile and target. Parker *et al.* [9] have shown that a differential range distribution may be decomposed to evaluate the extent of a variety of mechanisms.

In recent years this method has been used in studies of complete and incomplete fusion at energies from 60 to 150 MeV. These include ^{12}C on ^{51}V [9], ^{20}Ne and ^{22}Ne on ^{93}Nb [10,11], and the fissioning systems ^{16}O and ^{12}C on ^{238}U [12–14]. These data have been analyzed in terms of competing transfer reactions (and, where necessary, direct reactions and fission). For ^{12}C there are three dominant processes: complete fusion, ^8Be transfer, and α transfer. For ^{12}C on ^{51}V , Parker *et al.* [9] showed that effectively all of the cross section could be accounted for by these three processes up to an energy of 100 MeV and that, in turn, the yield of alpha particles in the reaction was accounted for by evaporation, alphas from decay of ^8Be following alpha transfer, and alphas of near beam velocity accompanying ^8Be transfer.

At the same time, Gadioli *et al.* [15] extended the excitation Omega code [16] for alpha-particle-induced reactions to calculate the kinematics and linear momentum transfer, and hence the differential range distribution of

spallation products in α -particle-induced reactions, and applied it successfully to the reaction $\alpha + {}^{59}\text{Co}$ (of interest because it yields the same compound system as ${}^{12}\text{C} + {}^{51}\text{V}$). It remained then to extend these calculations to the case of multiple cluster transfer from light-ion-induced reactions, which is the purpose of this work.

We report a twofold approach to the problem: experimental measurements of the ${}^{12}\text{C} + {}^{197}\text{Au}$ system at 10 MeV/nucleon and the development of a method of calculation for alpha cluster transfer reactions. We have measured the cross sections and differential range distributions of 22 spallation products. These data were then used to prepare a calculation of ${}^{12}\text{C}$ breakup and transfer from the projectile to the target. In addition to experimental detail and a full description of the model, we will demonstrate several conclusions:

(1) Incomplete fusion processes at these energies are by no means negligible, even for heavy targets with substantial Coulomb barriers. We find incomplete fusion events represent approximately 20% of the reaction cross section, including more than half of all nonfission events (approximately $\frac{2}{3}$ of the reaction cross section goes to fission, apparently nearly all following complete fusion).

(2) In order to account for the experimental data, it is essential to include preequilibrium emission from the complete fusion nucleus. Once again, this is not a negligible component; we estimate that, on the average, 0.61 neutron and 0.27 proton are emitted per event prior to equilibrium. Preequilibrium emission of charged particles is necessary, for example, to account for production of Po isotopes with full momentum transfer.

(3) As has been observed by a variety of authors [7,9,17–19] using several experimental techniques and theories, the transfer of ${}^8\text{Be}$ to the target is more important than that of a single α particle. Although this is not a surprising result, it must be viewed in the light of the extensive work on fission fragment angular correlations of Viola and co-workers [5,20,21], which seems to indicate that the fission channel is populated mainly by complete fusion and single alpha transfer, an approach we ourselves have been successful with in fission studies [13,14]. It remains unclear why spallation stems from, in addition to complete fusion, α and ${}^8\text{Be}$ transfer with the latter more important, while fission channels seem to tap principally the complete fusion and alpha transfer channels.

II. EXPERIMENTAL PROCEDURE AND RESULTS

Two types of experiment were performed in the external beam of the Variable Energy Cyclotron (VEC) of the U.K. Atomic Energy Authority (Harwell), using 120-MeV ${}^{12}\text{C}$ ions. These were incident upon Au targets with downstream Al catchers arranged in different geometries. The first experiment measured the production cross sections and, the second, the differential range distributions.

A. Cross sections

Two separate irradiations were performed, lasting 14 and 200 min, designed to detect the shorter- and longer-

TABLE I. Radioactive properties of residues measured.

Nuclide	Half-life (h)	γ ray (keV)	Branching ratio (%)
${}^{204}\text{Po}$	3.53	270.1	28.1
		884.0	30.3
		1016.3	24.4
${}^{203}\text{Po}$	0.612	893.5	19.0
		908.6	56.0
		1090.9	19.6
${}^{202}\text{Po}$	0.75	165.7	8.6
${}^{204}\text{Bi}$	11.2	688.6	50.0
		374.7	81.0
		899.2	98.5
${}^{203}\text{Bi}$	11.76	984.0	58.0
		820.2	29.6
		825.2	14.6
${}^{202}\text{Bi}$	1.72	896.9	13.1
		1847.3	11.5
		422.1	83.7
${}^{201}\text{Bi}^g$	1.80	657.5	60.6
		960.7	99.3
		629.1	24.3
${}^{200}\text{Bi}^g$	0.61	419.8	91.0
		462.3	98.0
		1026.5	100.0
${}^{203}\text{Pb}$	51.8	279.2	80.1
${}^{202}\text{Pb}^m$	3.53	422.1	85.5
		960.7	91.4
		331.2	78.7
${}^{201}\text{Pb}$	9.33	361.2	9.7
${}^{200}\text{Pb}$	21.5	147.6	37.7
		257.2	4.5
		268.4	4.0
${}^{199}\text{Pb}$	1.5	353.4	13.9
		1135.0	11.5
		173.4	24.0
${}^{198}\text{Pb}$	2.4	290.3	18.0
		365.4	19.0
		382.0	7.0
${}^{197}\text{Pb}^m$	0.74	865.3	8.0
		385.8	73.2
		167.4	10.6
${}^{201}\text{Tl}$	73.0	167.4	10.6
${}^{200}\text{Tl}$	26.1	367.9	87.2
		579.3	13.8
		1205.7	29.9
${}^{199}\text{Tl}$	7.4	208.2	12.2
		455.5	12.3
		282.8	28.0
${}^{198}\text{Tl}^m$	1.87	587.2	51.0
		636.7	55.0
		411.8	81.8
${}^{198}\text{Tl}^g$	5.3	636.7	10.1
		675.9	10.9
		152.2	7.23
${}^{197}\text{Tl}^g$	2.84	425.8	12.8
${}^{196}\text{Tl}^m$	1.4	695.4	41.0
${}^{196}\text{Au}$	148.3	333.0	22.9
		355.7	86.9
		426.1	7.20

lived nuclides. The target in each case consisted of a layer of gold evaporated onto a thick (relative to the range of spallation products) aluminum backing. The thickness of the gold layer, measured by Rutherford backscattering with the α beam of the Harwell van de Graaf accelerator, was determined to be $(3.24 \pm 0.08) \times 10^{18}$ and $(3.06 \pm 0.08) \times 10^{18}$ atoms/cm² in the two targets. Each target was mounted with the gold layer upstream inside an electrically suppressed Faraday cup and irradiated at a beam current of 300 nA. The beam intensity was monitored as a function of time during the irradiation.

Immediately after irradiation the target, including the backing, was removed and mounted 150 mm from the casing of a 25%-efficient Ge(Li) detector, which had been calibrated for energy and efficiency. Gamma-ray spectra of increasing duration were recorded over a period of several days. The GAMANAL code [22] was used to find and integrate the peaks in the spectra obtained. After correction for the absolute efficiency of the detector, decay curve analysis was performed on the peaks of interest (listed in Table I) to obtain production cross sections. The half-lives and branching ratios, listed in the table, were taken from the Gesellschaft für Schwerionenforschung mbH (GSI) compilation [23], with the exception of the branching ratios for the decay of ¹⁹⁸Pb, which were taken from the table of isotopes of Ref. [24] because the ratio of γ -ray intensities in our data was much more consistent with those than with the GSI values. In cases

where the yield of the same nuclide could be determined from several different γ -ray lines or from both the short and long experiment, the results obtained from the different sources were in good agreement.

A complication of this work is that most of the nuclides detected include substantial contributions to their yield due to feeding by shorter-lived precursors. In most cases the half-lives of the precursors are too short for this feeding to be directly observable (although considerable feeding occurred during the 200-min irradiation), so that the yields of the precursors could not be separately quantified, and the measured activity of the observed daughter must be taken to include the yield of the precursors. On the other hand, the half-life of the precursor is not in general short enough to be negligible. Under these conditions standard decay curve analysis leads to a deduced cross section equal to $\sigma_D + [\lambda_P / (\lambda_P - \lambda_D)] \sigma_P$, where σ_D and σ_P are the true cross sections for production of the detected daughter and precursor, respectively, and λ_D and λ_P are their decay constants. This formula can also be extended to the case where the detected nuclide contains a contribution due to several-stage feeding from a grandparent. We list in Table II, for each detected nuclide, the measured cross section as well as the contributions to its yield due to these feeding processes. In cases where feeding from precursors occurs, the tabulated cross section represents a complicated weighted sum of the production cross sections for the observed product

TABLE II. Cross section and precursor contributions for measured nuclides.

Residue	Contribution to nuclide production	Cross section (mb)
²⁰⁴ Po	²⁰⁴ Po + ²⁰⁴ At	6.7 ± 0.7
²⁰⁴ Bi	²⁰⁴ Bi + 1.46 ²⁰⁴ Po + 1.4 ²⁰⁴ At	7.6 ± 0.4
²⁰³ Po	²⁰³ Po + 0.88 ²⁰³ At	30 ± 1
²⁰³ Bi	²⁰³ Bi + 1.04 ²⁰³ Po + 0.69 ²⁰³ At	41 ± 5
²⁰³ Pb	²⁰³ Pb + 1.29 ²⁰³ Bi + 1.29 ²⁰³ Po + 0.89 ²⁰³ At	73 ± 3
²⁰² Po	²⁰² Po + 0.91 ²⁰² At	140 ± 8
²⁰² Bi	²⁰² Bi + 1.72 ²⁰² Po + 1.51 ²⁰² At	280 ± 15
²⁰¹ Bi ^g	²⁰¹ Bi ^g + 1.145 ²⁰¹ Po ^g + 1.141 ²⁰¹ Po ^m + 0.33 ²⁰¹ At	100 ± 30
²⁰¹ Pb	²⁰¹ Pb + 1.12 ²⁰¹ Bi ^m	
	+ 1.24 ²⁰¹ Bi ^g + 1.25 ²⁰¹ Po ^g + 1.23 ²⁰¹ Po ^m + 0.36 ²⁰¹ At	150 ± 5
²⁰¹ Tl	²⁰¹ Tl + 1.14 ²⁰¹ Pb + 1.16 ²⁰¹ Bi ^{g+m}	
	+ 1.16 ²⁰¹ Po ^{g+m} + 0.33 ²⁰¹ At	140 ± 7
²⁰⁰ Po	²⁰⁰ Po + 0.5 ²⁰⁰ At	11 ± 5
²⁰⁰ Bi	²⁰⁰ Bi + 1.26 ²⁰⁰ Po + 0.6 ²⁰⁰ At + 0.059 ²⁰⁴ At	111 ± 7
²⁰⁰ Pb	²⁰⁰ Pb + 1.03 ²⁰⁰ Bi + 0.89 ²⁰⁰ Po + 0.42 ²⁰⁰ At + 0.044 ²⁰⁴ At	160 ± 20
¹⁹⁹ Bi	¹⁹⁹ Bi + 1.1 ¹⁹⁹ Po ^g + 0.72 ¹⁹⁹ Po ^m + 0.42 ²⁰³ At	120 ± 15
¹⁹⁹ Pb	¹⁹⁹ Pb + 1.43 ¹⁹⁹ Bi + 1.34 ¹⁹⁹ Po ^g + 0.64 ¹⁹⁹ Po ^m + 0.48 ²⁰³ At	150 ± 20
¹⁹⁹ Tl	¹⁹⁹ Tl + 1.25 ¹⁹⁹ Pb + 1.33 ¹⁹⁹ Bi + 0.81 ¹⁹⁹ Po ^m + 1.17 ¹⁹⁹ Po ^g	
	+ 0.015 ²⁰³ Po + 0.41 ²⁰³ At	199 ± 10
¹⁹⁸ Pb	¹⁹⁸ Pb + 1.09 ¹⁹⁸ Bi + 0.33 ¹⁹⁸ Po + 0.03 ²⁰² Po + 0.17 ²⁰² At	45 ± 10
¹⁹⁸ Tl ^g	¹⁹⁸ Tl ^g + 0.68 ¹⁹⁸ Tl ^m + 1.83 ¹⁹⁸ Pb + 1.83 ¹⁹⁸ Bi + 0.55 ¹⁹⁸ Po	
	+ 0.036 ²⁰² Po + 0.27 ²⁰² At	134 ± 7
¹⁹⁸ Tl ^m	independent yield	66 ± 4
¹⁹⁷ Pb ^m	¹⁹⁷ Pb ^m + 1.24 ¹⁹⁷ Bi + 0.91 ²⁰¹ At + 0.037 ²⁰¹ Po ^m + 0.025 ²⁰¹ Po ^g	48 ± 3
¹⁹⁷ Tl	¹⁹⁷ Tl + 1.33 ¹⁹⁷ Pb + 1.4 ¹⁹⁷ Bi + 0.99 ²⁰¹ At	176 ± 10
¹⁹⁷ Hg ^m	independent yield	36 ± 2
¹⁹⁶ Tl ^m	independent yield	16.5 ± 5
¹⁹⁶ Au	independent yield	145 ± 10

and its precursors. While this may appear to be a quantity lacking in physical significance, it is, nevertheless, the measured quantity and the only absolute value obtainable. These cross sections and corresponding recoil distributions will, in succeeding sections, be compared with the values calculated from the proposed model which represent the same weighted sums as listed in Table II.

B. Range distributions

The recoil range distributions of the 22 nuclides listed in Table I were measured by irradiating a thin gold target backed by a stack of thin aluminum catchers. The target consisted of about $50 \mu\text{g}/\text{cm}^2$ of gold evaporated onto Al of thickness $100 \mu\text{g}/\text{cm}^2$. The catcher stack used to define the differential range measurements comprised 18 self-supporting foils of Al, each $40 \mu\text{g}/\text{cm}^2$ thick, mounted immediately behind the target. The thickness of each catcher foil was determined to an accuracy of 5% by measuring the energy lost by 5.8-MeV alpha particles from ^{244}Cm in traversing the foil. The whole of the target assembly was mounted inside an electrically suppressed Faraday cup. The target assembly was irradiated for a period in excess of 6 h at an average beam intensity of 225 nA, corresponding to an integrated beam of 5×10^{15} particles.

After irradiation the target and each of the catcher

foils was counted over a period of several weeks on the face of one of two 25%-efficient Ge(Li) detectors whose energy calibration and absolute efficiency were known. The resulting γ -ray spectra were then analyzed using the same procedures as described above.

The recoil range distribution for each nuclide was then obtained by dividing the yield in each foil by the thickness of that foil, with a correction applied for the relative efficiencies of the two detectors used. This distribution for each nuclide was then normalized to the total production cross section of that nuclide, measured as described above.

The recoiling residual nuclei (from complete fusion or incomplete fusion) lose energy when passing through the $50\text{-}\mu\text{g}/\text{cm}^2$ Au target; therefore, the experimental ranges are smeared by an amount corresponding to that thickness of aluminum producing the same energy loss as $50 \mu\text{g}/\text{cm}^2$ of gold. From the range-energy tables of Northcliffe and Schilling [25], it is easy to show that the smearing of the range of a nuclide produced by complete fusion is about $10 \mu\text{g}/\text{cm}^2$, for a ^8Be transfer about $7 \mu\text{g}/\text{cm}^2$, and for α transfer $4 \mu\text{g}/\text{cm}^2$. In each case this represents about 3% of the measured range. The experimental range distributions for Po, Bi, Pb, and Tl are shown in Figs. 1–4, respectively, as the solid-line histograms.

III. THEORETICAL CALCULATIONS

Examination of the experimental recoil range distributions immediately reveals the presence of at least three different contributing mechanisms producing residues with different average ranges: one at about $350 \mu\text{g}/\text{cm}^2$, one at about $200 \mu\text{g}/\text{cm}^2$, and one at about $50\text{--}100 \mu\text{g}/\text{cm}^2$. A closer inspection, considering only the independent yields which contribute to the measured distributions, indicates that the At and Po isotopes have the maximum observed average range, the Bi and Pb isotopes have mostly the intermediate average range, and the Tl isotopes have the smallest average range. The apparent explanation of these findings consists in assuming that the three mechanisms essentially correspond to the complete fusion of the projectile with the target, to the incomplete fusion of a ^8Be or two α 's with the target, and finally to the fusion of a single α particle with the target. This hypothesis is based on the fact that these three mechanisms would produce residues with the observed average recoil ranges. In addition, the theoretical calculations indicate that even accounting for preequilibrium emission of protons and evaporation of either protons or α particles it would be difficult to explain, by assuming only occurrence of complete fusion processes, the quite sizable cross section for production of Bi, Pb, and Tl isotopes one observes. Previous investigations [7,9,17] also indicated the necessity of the two incomplete fusion processes to explain the production of residues with charge smaller by more than one unit than the charge of the compound nucleus produced in the complete fusion process; however, observation of the recoil distribution of the residues produced seems to constitute a more direct proof of these processes.

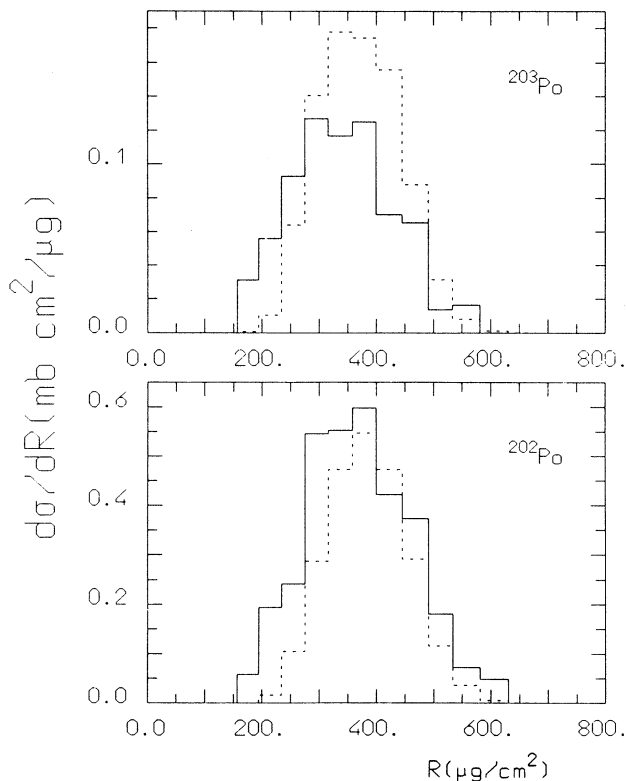


FIG. 1. Experimental (solid line) and calculated (dashed line) histograms of the differential recoil range distributions for Po isotopes.

We have developed a code to reproduce the present data in terms of contributions from three distinct processes: complete fusion, ^8Be transfer, and α -particle transfer. These calculations are discussed in the following sections.

A. Complete fusion

The yields of the isotopes which contribute to the complete fusion component of the observed recoil distributions were initially calculated assuming that the compound nucleus ^{209}At would deexcite only by evaporation and fission. The calculation is described later; however, we may anticipate that using average level-density parameters from the Fermi-gas model [$a = A/8$ (MeV^{-1})], realistic inverse cross sections for nuclei in this mass region (in our code we use semiclassical expressions [26] with parameters that reproduce the values of the inverse cross sections calculated by the optical model at an energy of about 20–30 MeV), the experimental binding energies from Wapstra and Audi [27], and pairing energies

from Nemirovski and Adamchuck [28], we could not obtain a reasonable reproduction of all the measured distributions.

Shell corrections to the level-density parameters do not suffice to remove these discrepancies. We assumed that this correction should be considered for nuclei within 4 units of $Z=82$ or $N=126$ closed shell and below 20 MeV of excitation energy, where the level-density parameter was considerably reduced. This reduction was estimated from the known a from slow neutron resonance spacing, assuming that the shell correction should disappear above 20 MeV of excitation energy. A few examples of the discrepancies between the experimental data and the theoretical calculations are shown in Fig. 5.

A very reasonable reproduction of all the data could be obtained by allowing for the preequilibrium emission of fast neutrons or protons, however. The average number of these preequilibrium neutrons and protons and their spectra were evaluated by solving a set of Boltzmann master equations as described by Fabrici *et al.* [29] (using the same parameters, the only difference being the bind-

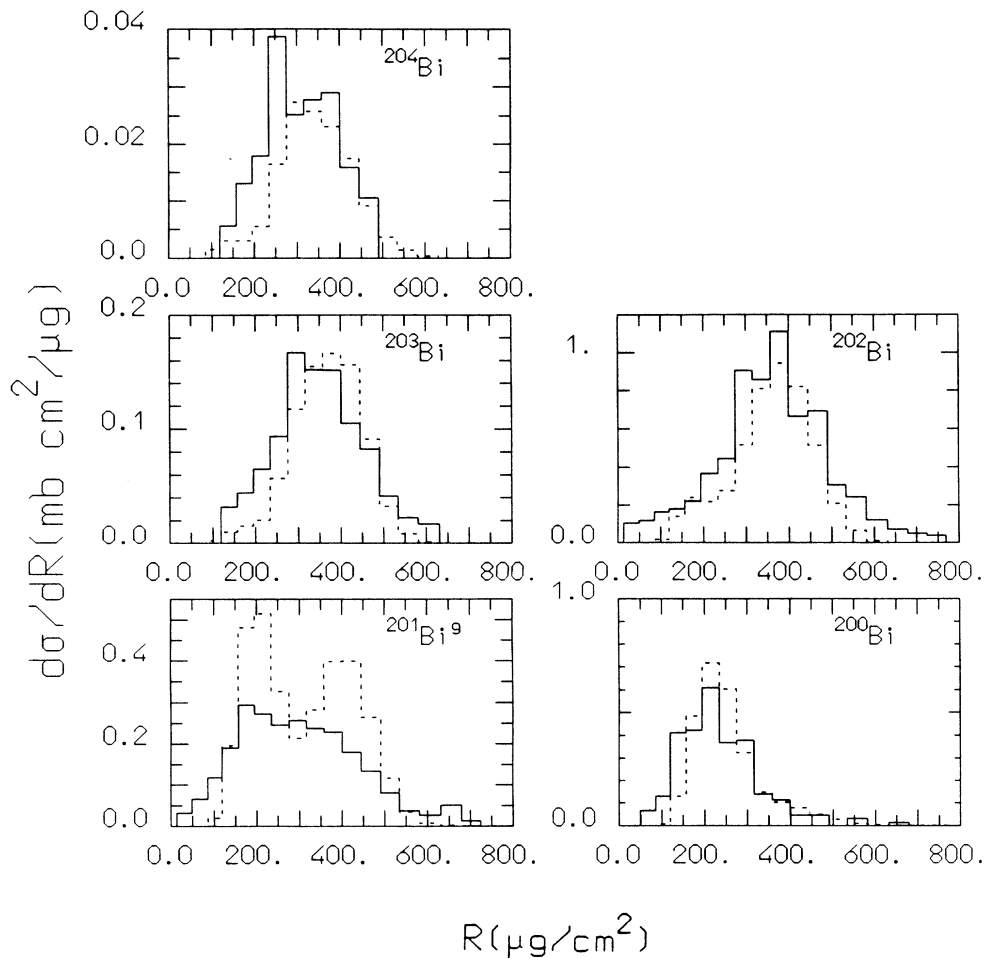


FIG. 2. As in Fig. 1, for the Bi isotopes.

ing energies appropriate to the case here considered). We estimated that the average multiplicity of these preequilibrium particles is equal to 0.61 for the neutrons and 0.27 for the protons. To take into account the possibility of these emissions, we modified the code described by Gadioli *et al.* [15,30] by replacing the part which evaluates the probability of preequilibrium emission (that in the original version was based on the exciton model) with a new one where the probability of emission of a fast neutron or proton is estimated by equating the probability of emission of these particles to the calculated average multiplicities and estimating their energy using the calculated spectra and the extraction of random numbers as described by Dostrovsky, Fraenkel, and Friedlander [26].

B. Incomplete fusion

To evaluate the energy distributions of the nuclei produced in the incomplete fusion processes, we schematized this process as an elastic breakup of the projectile followed by the absorption of one of the fragments by the target nucleus.

To evaluate the energy and angular distribution for the emitted fragment, we adopted the following procedure. The incident projectile P was assumed to be slowed by the Coulomb barrier between the projectile and target. The remaining energy E_p was divided between the two fragments using the Serber approximation [31] generalizing the expression given by Matsuoka *et al.* [32]:

$$\frac{d^2\sigma}{dE_a d\Omega_a} \propto \frac{\sqrt{E_a E_b}}{[2\mu B_p + 2m_a^2 E_p / m_p + 2m_a E_a - 4(m_a^3 E_p E_a / m_p)^{1/2} \cos\theta]^2}, \quad (1)$$

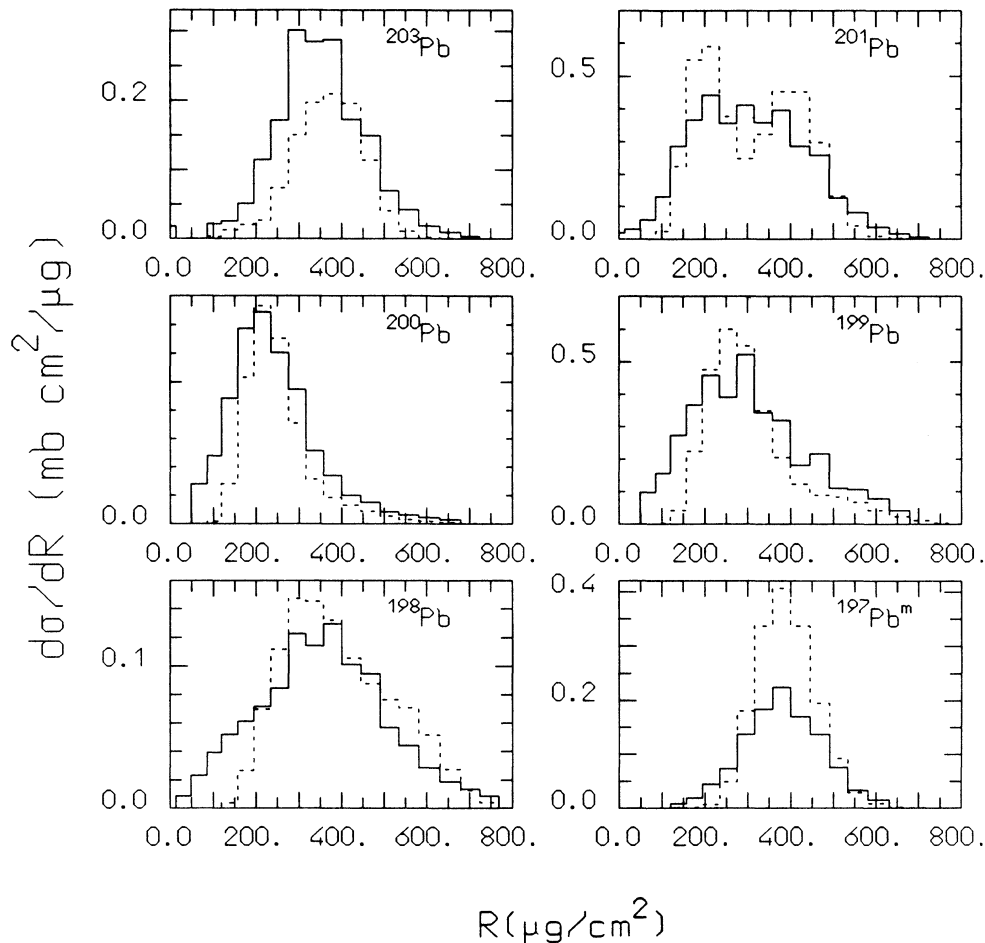


FIG. 3. As in Fig. 1, for the Pb isotopes.

where it is the fragment a which flies away and the fragment b which fuses with the target, E_a and E_b are their kinetic energies, B_p is the binding energy of a and b in P , μ is the reduced mass of the system $a + b$, m_p , m_a , and m_b are the masses of P , a , and b , and θ is the emission angle of a with respect to the direction of P . Finally, the emitted fragment is accelerated by the Coulomb field of the nucleus after absorption of the complementary fragment.

This procedure is certainly very approximate; in fact, at such low incident energies one should expect considerable distortions of the incident projectile and emitted fragment wave functions. However, this simple procedure allows reproduction of the fragment spectra sufficiently accurately for our purposes. This is shown in Fig. 6 for the case of a similar reaction at comparable energy (C fragments emitted in the breakup to ^{20}Ne ions bombarding ^{93}Nb at 148 MeV incident energy [11]).

Once the probability of emission of the fragment, as a function of both the angle and energy is evaluated, the energy and angular distribution of the intermediate excit-

ed system created in the incomplete fusion of the complementary fragment is estimated by the usual Monte Carlo procedure of selecting, through extraction of random numbers, the angle of emission of the fragment and by subtracting a randomly selected value of its energy from the maximum possible value. The excited nuclei following absorption of either the ^8Be ion or α then deexcite by evaporation.

C. Recoil distributions

A detailed description of the computational procedure has been reported elsewhere [15,30]. However, we summarize here, for completeness, how the recoil range distribution of the residues is evaluated.

The recoil direction of the residues was followed during the deexcitation chain starting from the initial direction of the composite nucleus produced in the projectile-target nucleus interaction. This was the beam direction for complete fusion or the recoil direction after the projectile breakup and partial fusion in the case of incom-

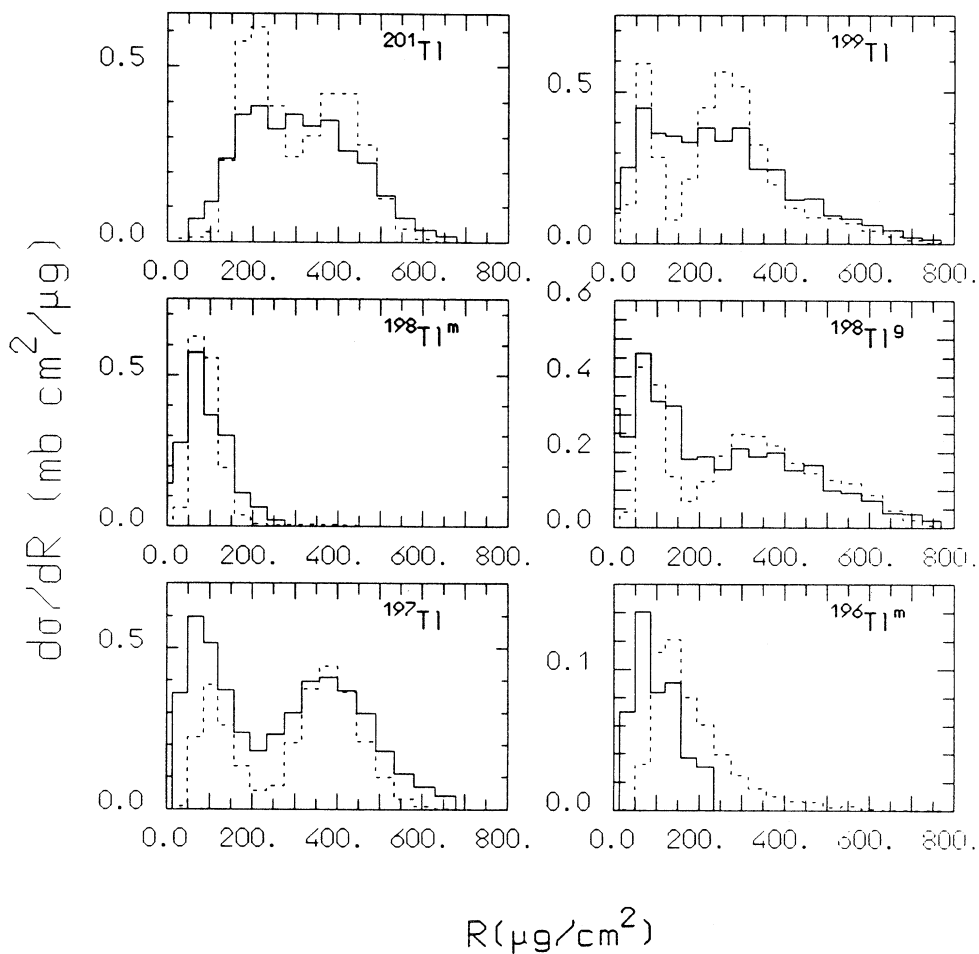


FIG. 4. As in Fig. 1, for the Tl isotopes.

plete fusion processes.

The angular distribution of the neutrons or protons emitted in the preequilibrium phase was assumed to be given by [33,34]

$$\frac{d^2\sigma}{dE d\Omega} \propto \exp(-\theta/\Delta\theta), \quad (2)$$

where

$$\Delta\theta = \frac{2\pi}{kR_{CN}}, \quad (3)$$

and R_{CN} is the composite nucleus radius, given by $R_{CN} = 1.25 A_{CN}^{1/3}$, and k is the wave number of the emitted particle.

The evaporated particles were assumed to have an isotropic angular distribution in the reference frame of the decaying nucleus except at the end of the evaporation cascade (when the decaying system may still have considerable angular momentum and the angular momentum of the evaporated particle has a high probability to be

aligned with it), where a $1/\sin\theta$ angular distribution was assumed (θ is the angle between the direction of the recoiling nucleus before the considered emission and the direction of the evaporated particle). In the results of the calculations presented later, the anisotropic distribution was assumed to occur at excitation energies below about 25 MeV.

After each emission the change in the direction of the recoiling nucleus was evaluated and the final result of the cascade was a residual nucleus identified by Z and A , with a momentum \mathbf{p} . The corresponding range was evaluated by a third-order polynomial fit to the linear momentum-range tabulations of Northcliffe and Schilling [25]. Finally, the range was projected onto the beam axis for comparison with experiments. The change in direction for the residual nucleus along the deexcitation chain is far from negligible and in fact reflects in a considerable broadening of the recoil distributions.

The target thickness was taken into account by assuming that the interaction of the projectile with the target nucleus could occur with equal probability at any depth

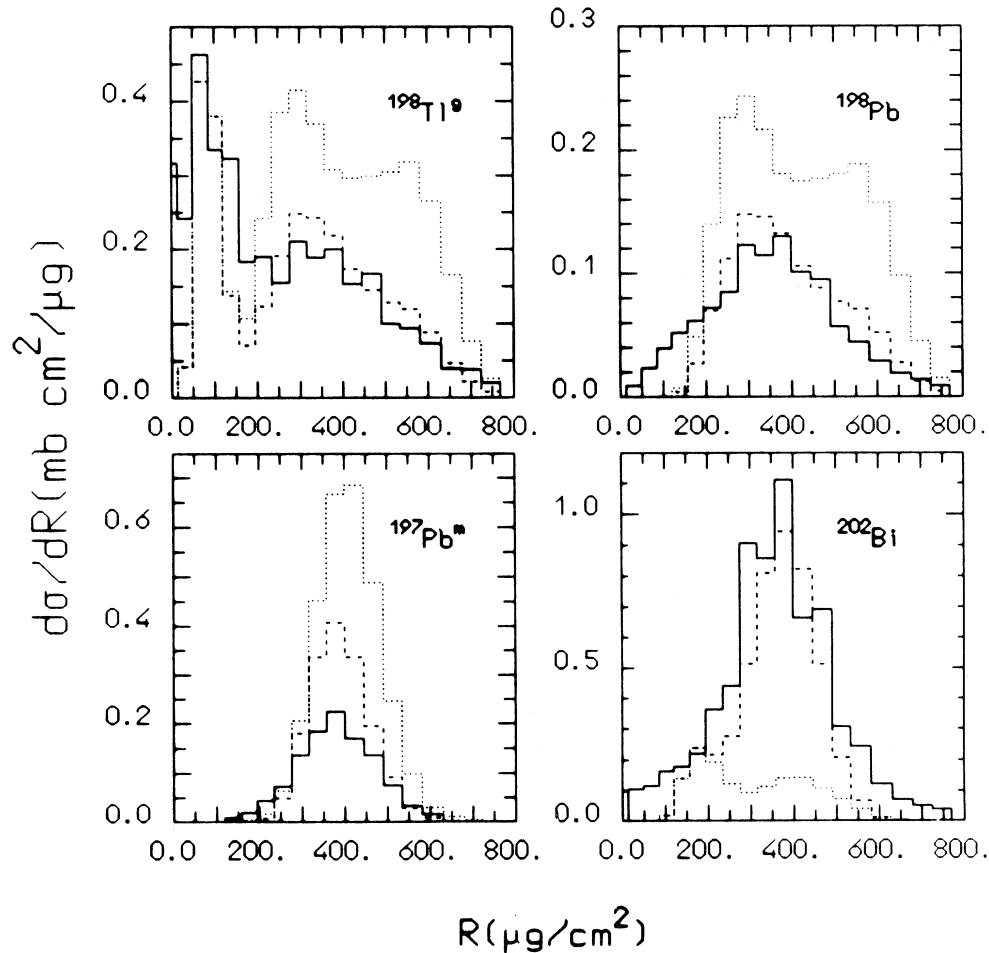


FIG. 5. Recoil distributions calculated *without* (dotted-line histograms) and *with* (dashed-line histograms) inclusion of preequilibrium emission of fast nucleons in complete fusion are compared with the experimental distributions (solid-line histograms).

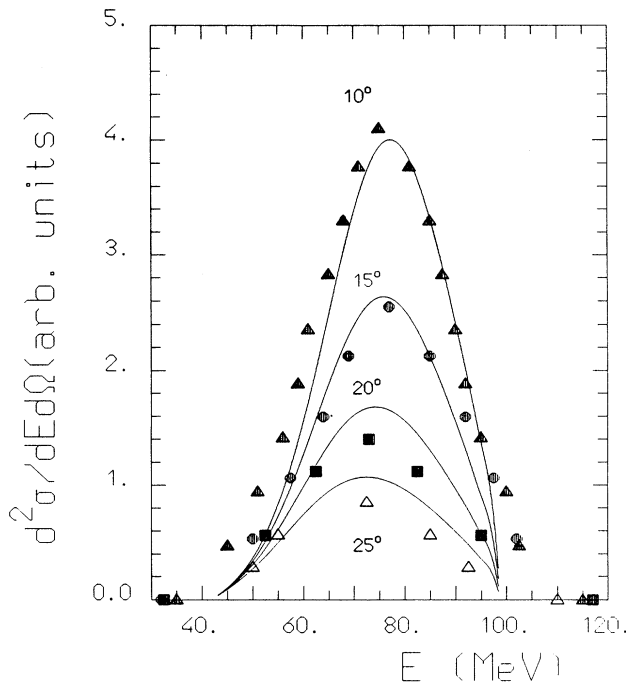


FIG. 6. Comparison of experimental (solid and open triangles, solid circles and squares) and calculated (solid lines) double differential spectra for the emission of C in the reaction $^{20}\text{Ne} + ^{93}\text{Nb}$ at 148 MeV (data from Ref. [11]).

within the target. The consequent broadening of the calculated range distributions is rather small. Straggling was not taken into account mainly because of the lack of experimental information for the fragments produced in this reaction.

D. Effect of fission

Various experiments [1,5] indicate that ^{209}At , produced in the complete fusion process, ultimately fissions in a large fraction of cases. One may evaluate (and our code does so) the probability of fission during the evaporation chain only with a detailed knowledge of the fission barriers of the nuclei of the chain as a function of both the nuclear mass A and the angular momentum J . In this mass region such knowledge is very scanty. Therefore, instead of evaluating explicitly the probability of fission, the following procedure was adopted. Consider a randomly selected deexcitation path of an equilibrated nucleus A produced in a complete fusion process:

$$A \rightarrow B \rightarrow C \rightarrow \dots$$

B, C, \dots are the nuclei reached during the deexcitation chain, each with a given energy, linear, and angular momentum. The probability of this particular decay sequence is

$$\mathcal{P} = \left(\frac{\Gamma_p^A}{\Gamma_p^A + \Gamma_f^A} \frac{\Gamma_p^B}{\Gamma_p^B + \Gamma_f^B} \frac{\Gamma_p^C}{\Gamma_p^C + \Gamma_f^C} \dots \right) \times \left(\frac{\Gamma_i^A}{\Gamma_p^A} \frac{\Gamma_{i'}^B}{\Gamma_p^B} \frac{\Gamma_{i''}^C}{\Gamma_p^C} \dots \right), \quad (4)$$

where $\Gamma_p^{A,B,C}$, $\Gamma_f^{A,B,C}$, and $\Gamma_{i,i',i''}^{A,B,C}$ are, respectively, the total decay rates of A , B , and C for particle emission, fission, and emission of the particular particles emitted in the considered sequence.

In a Monte Carlo calculation one samples a great number of possible decay sequences, and at the end, one estimates the average value of the probability (4). If the two terms in the right-hand side of (4) are *independent* of each other, the average probability becomes

$$\bar{\mathcal{P}} = (1 - \bar{P}_f) \left(\frac{\Gamma_i^A}{\Gamma_p^A} \frac{\Gamma_{i'}^B}{\Gamma_p^B} \frac{\Gamma_{i''}^C}{\Gamma_p^C} \dots \right), \quad (5)$$

where \bar{P}_f is the average probability of fission and the second factor in (5) is the quantity one evaluates in a Monte Carlo calculation which does not explicitly take into account the fission option.

A simple way to decide if the two terms in (4) are or are not statistically independent is to look to the probability of fission as a function of the energy for the reaction considered. Varying the incident energy, one samples different nuclei during the various deexcitation chains. Taking into account that in the majority of the cases the nuclei excited in the reaction decay either by emitting a neutron or fissioning, the nuclei sampled when one varies the incident energy or varies the decay sequence are essentially the same (even if the probability of reaching one of them is different in the two cases). If the probability of fission displays a weak energy dependence which is smoothly varying, one may safely conclude that the probability of fission is largely independent of the particular sequence of decays and thus the two terms in (4) are statistically independent.

Since the fission probability for the $^{12}\text{C} + ^{197}\text{Au}$ reaction is essentially constant with varying incident energy between about 90 and 120 MeV [1], it may be concluded that the cross section for producing a particular residue may be evaluated without explicitly considering the probability of fission if, in the calculation, one substitutes for the cross section for complete fusion, σ_{cf} the product $\sigma_{\text{cf}}(1 - \bar{P}_f)$.

E. Comparison with the data and estimate of the partial cross sections for complete and incomplete fusion

The only free parameters in the calculation were the three cross sections $\sigma_{\text{cf}}(1 - \bar{P}_f)$ for complete fusion without fission, σ_{Be} for incomplete fusion of a ^8Be fragment, and σ_α for incomplete fusion of a single α particle. All the other input parameters had, as stated above, the values suggested by previous, independent analyses of other experimental data. The dashed-line histograms in Figs. 1–4 give the calculated recoil range distributions

assuming for the three cross sections the values $\sigma_{cf}(1-\bar{P}_f)=350$ mb, $\sigma_{8\text{Be}}=260$ mb, and $\sigma_{\alpha}150$ mb.

The main features of most of the measured distributions are reproduced satisfactorily by the calculation, in particular the location of the maxima, the widths of the distributions, and the absolute cross sections. In particular, the ability of the calculation to reproduce the absolute cross sections is illustrated in Fig. 7, where the ratios of the experimental to the calculated total cross sections for production of various isotopes are shown. Most of the cross sections are reproduced within 30%, which appears to be remarkable accuracy.

For a few nuclei, in particular the $A=201$ isobars, the calculated distributions appear more structured than the measured ones. This is partly due to neglect of straggling in the calculations, but may also reflect our extreme schematization of the incomplete fusion processes. While our procedure seems to be to a large extent justified by the comparison with experiment, it is certainly true that other incomplete fusion processes will occur in practice. Thus, not only ^8Be will fuse with gold, but also the other Be isotopes such as ^7Be or ^9Be . Consideration of these processes would smear the calculated distributions, reducing the discrepancies with the data. However, perhaps with the exception of the $^{201}\text{Bi}^g$ recoil distribution, which is characterized by the largest experimental uncertainties (the error on the absolute cross sections is estimated to be greater than 25%, reflecting not statistical uncertainty as much as difficulty in measurement), we feel that one may conclude that a substantially correct description of the processes occurring has been achieved. In Table III the calculated contribution of each mecha-

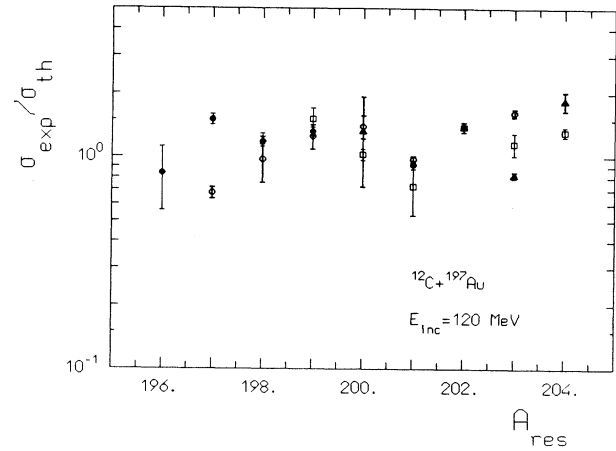


FIG. 7. Ratio of the experimental cross section to that calculated, for all the spallation products ($^{198}\text{Tl}^m$, cross, other Tl isotopes, solid circles, Pb isotopes, open circles, Bi isotopes, open squares, Po isotopes, solid triangles).

nism (the complete and the two incomplete fusion processes) to the cumulative production of each residue is given, and Fig. 8 shows, as an example, the independent contributions to the cumulative recoil distribution of $^{198}\text{Tl}^g$.

Adding to the three cross sections for complete and incomplete fusion the fission cross section [1] (≈ 1220 mb), one finds for the reaction cross section σ_R a value of about 1980 mb, which compares very favorably with the value calculated by Thomas [35] (2099 mb).

TABLE III. Contribution of the three processes to the calculated cross section.

Nuclide	σ_{expt}	$\sigma_{\text{th}}^{\text{cf}}$	$\sigma_{\text{th}}^{\text{Be}}$	$\sigma_{\text{th}}^{\alpha}$	$\sigma_{\text{th}}^{\text{tot}}$
^{204}Po	6.7 ± 0.7	3.63	0.00	0.00	3.63
^{203}Po	30.0 ± 1	36.43	0.00	0.00	36.43
^{202}Po	140.0 ± 8	101.25	0.00	0.00	101.25
^{200}Po	11.0 ± 5	8.31	0.00	0.00	8.31
^{204}Bi	7.60 ± 0.4	5.25	0.53	0.00	5.79
^{203}Bi	41.0 ± 5	33.77	1.72	0.00	35.49
^{202}Bi	280.0 ± 15	174.70	27.60	0.00	202.30
$^{201}\text{Bi}^g$	100.0 ± 30	74.22	63.26	0.00	137.49
^{200}Bi	111.0 ± 7	15.96	92.20	0.00	108.16
^{199}Bi	120.0 ± 15	28.18	51.16	0.00	79.33
^{203}Pb	73.0 ± 3	42.73	2.26	0.00	44.99
^{201}Pb	150.0 ± 5	80.64	73.04	0.00	153.68
^{200}Pb	160.0 ± 20	15.02	99.65	0.00	114.67
^{199}Pb	150.0 ± 20	43.50	76.01	0.00	119.51
^{198}Pb	45.0 ± 10	41.68	4.54	0.00	46.22
$^{197}\text{Pb}^m$	48.0 ± 3	70.86	0.00	0.00	70.86
^{201}Tl	140.0 ± 7	75.70	75.88	0.86	152.44
^{199}Tl	199.0 ± 10	41.62	72.13	36.91	150.66
$^{198}\text{Tl}^g$	134.0 ± 7	68.97	9.25	35.18	113.4
$^{198}\text{Tl}^m$	66.0 ± 4	0.025	2.37	51.73	54.13
^{197}Tl	176.0 ± 10	75.65	4.03	37.22	116.90
$^{196}\text{Tl}^m$	16.5 ± 5	0.63	1.88	17.17	19.68

Bimbot, Gardes, and Rivel [7] have estimated the cross section for incomplete fusion of a ^8Be fragment between 60 and 90 MeV incident ^{12}C energy. Their estimated values are given in Fig. 9 by the solid line (they include also the contribution of complete fusion processes followed by evaporation of one α particle). Our value at 120 MeV is perfectly compatible with their estimates (for consistency we have added to the value of 260 mb given above the calculated cross section for one alpha-particle evaporation from ^{209}At , which amounts to 51 mb). These authors have also estimated the cross section for incomplete fusion of one α particle by the measured yield of Tl isotopes. Since transfer of two protons might also contribute to the yield of Tl isotopes, with mass smaller than 199 (they found evidence for this process by studying the $^{12}\text{C} + ^{209}\text{Bi}$ reaction at the same energies), their value of σ_α estimated by summing the production cross sections of Tl isotopes, must be considered an upper limit. Even then, their values of σ_α , shown also in Fig. 9, are substantially smaller than the corresponding $\sigma_{^8\text{Be}}$, as is our estimate.

It is to be noted that, while we do not need to include two-proton incomplete fusion for reproducing satisfactorily the yield of the Tl isotopes with mass smaller than 199, a contribution from such a process cannot be excluded (for instance, the smallest recoil component to the ^{197}Tl and $^{196}\text{Tl}^m$ distributions peaks experimentally at a value slightly smaller than the calculated one, a fact which could be due to our neglect of two-proton transfer processes). Thus our value also is strictly speaking, an upper limit on the true σ_α .

Finally, our estimate for incomplete fusion cross sections (260 and 150 mb) appear to be consistent with those reported recently by Tserruya *et al.* [19] for ^{12}C bombardment of ^{160}Gd .

IV. SUMMARY

In this paper we have presented the results of the measurement of recoil ranges of 22 residues produced in the interaction of ^{12}C ions with ^{197}Au at 120 MeV. The technique based on the distribution of γ activities found in

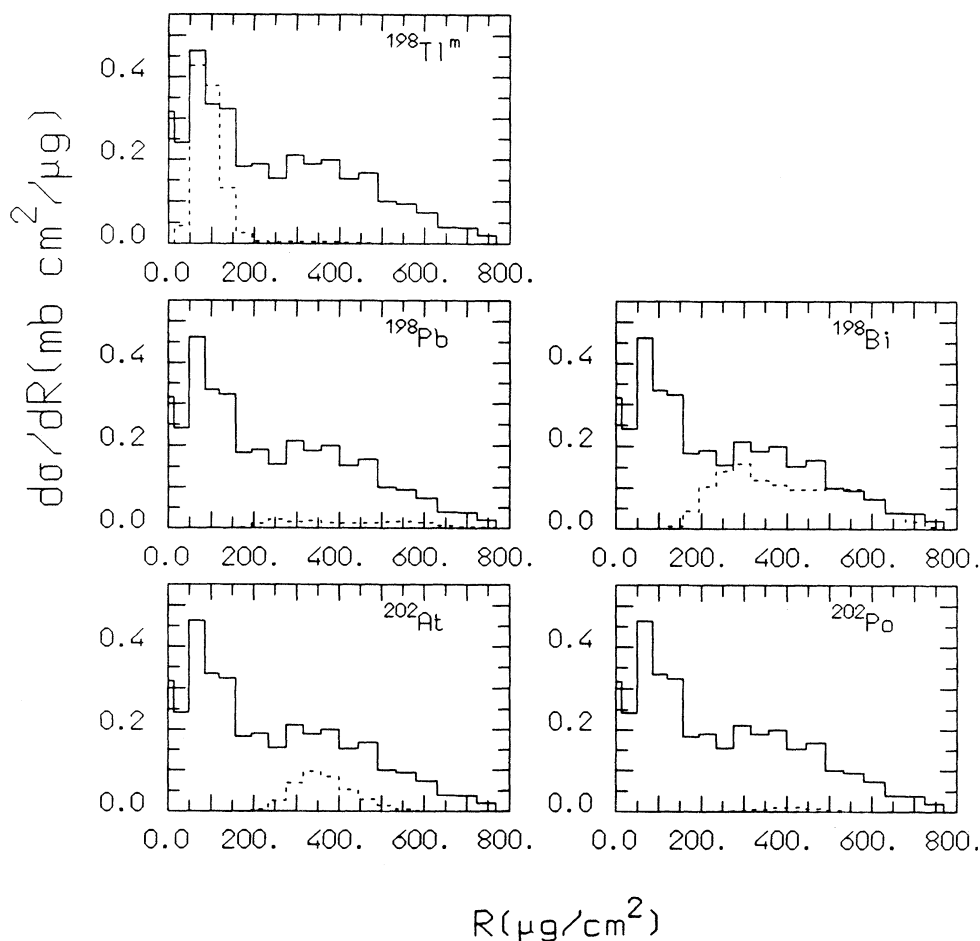


FIG. 8. Calculated recoil distributions of $^{198}\text{Tl}^m$ (independent production) and of precursors contributing to the cumulative distribution of $^{198}\text{Tl}^m$. The measured cumulative distribution is given by the solid-line histograms.

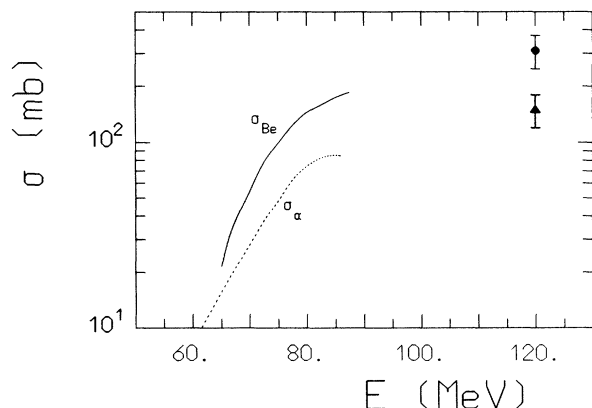


FIG. 9. Cross section for the transfer of ${}^8\text{Be}$ and α particles found in this work (circle and triangle) and the measurements of Bimbot, Gardes, and Rivet [7] (solid and dashed lines).

thin Al absorbers downstream from a thin target allows the direct identification of product nuclei from either complete or incomplete fusion events.

We have introduced a method of calculation of their production cross sections and range distributions taking account of complete fusion as well as the transfer of a single α and a ${}^8\text{Be}$ fragment from ${}^{12}\text{C}$ to the target. The mechanism of these processes was assumed to be elastic breakup followed by absorption of one of the fragments by the target.

We have found that the recoil distributions of residues produced in complete fusion events could only be reproduced by allowing for preequilibrium emission of about 0.9 fast nucleons (≈ 0.6 neutron and 0.3 proton) per complete fusion event. The experimental range distributions are reproduced quite well by the calculation; in many cases several different reaction pathways are necessary to describe the overall production of a single nuclide. This result emphasizes the power of the recoil technique to

isolate competing mechanisms in the reaction studied.

The experimental results of Bimbot, Gardes, and Rivet [7], together with ours, indicate that incomplete fusion processes begin from an incident energy near the projectile-target Coulomb barrier (≈ 58 MeV), rising monotonically at least up to 120 MeV, in agreement with the findings of Tserruya *et al.* [19].

As suggested in previous papers [7,17,19], we find ${}^8\text{Be}$ transfer to be more important than transfer of a single α particle; the ${}^8\text{Be}$ and α transfer reactions account for 260 and 150 mb, respectively. The nonfission cross section is about 760 mb, of which less than half (350 mb) is complete fusion. The preequilibrium n - and p -emission yields are about 215 and 95 mb, respectively. The estimated evaporated α yield is about 75 mb, while that of fast α particles from breakup processes is about 560 mb.

A detailed comparison of these data with existing theories of incomplete fusion is outside the scope of this work. In our opinion, for such a comparison to be really meaningful, data from a variety of target nuclei interacting with several different light ions ranging in energy to several tens of MeV/nucleon must be available. While several range studies at $E \leq 10$ MeV/nucleon have been performed and double differential light particle spectra are widely available, there are few measurements of the yields of or momentum transfer to residual nuclei at $E \geq 10$ MeV/nucleon. It is hoped that in the near future, we can, ourselves, contribute such experimental data.

ACKNOWLEDGMENTS

The work described in this paper was undertaken as part of the Underlying Research Programme of the United Kingdom Atomic Energy Authority. We thank M. Miller who produced all the target and catcher foil used, Dr. J. Asher, and Prof. P. Guazzoni and Prof. L. Zetta for enlightening discussions. J.J.H. was supported by the Natural Sciences and Engineering Research Council of Canada and by a travel grant from NATO.

*Present address: School of Physics and Space Research, University of Birmingham, Edgbaston, Birmingham B15 2TT, U.K.

- [1] G. E. Gordon, A. E. Larsh, T. Sikkeland, and G. T. Seaborg, *Phys. Rev.* **120**, 1341 (1960).
- [2] T. D. Thomas, G. E. Gordon, R. M. Latimer, and G. T. Seaborg, *Phys. Rev.* **126**, 1805 (1962).
- [3] R. Bimbot, M. Lefort, and A. Simon, *J. Phys. (Paris)* **29**, 563 (1968).
- [4] J. D. Stickler and K. J. Hofstetter, *Phys. Rev. C* **9**, 1064 (1974).
- [5] T. Sikkeland and V. E. Viola, in *Proceedings of the International Conference on Heavy Ion Reactions*, Asilomar, California, 1964 (unpublished).
- [6] H. C. Britt and A. R. Quinton, *Phys. Rev.* **124**, 877 (1961).
- [7] R. Bimbot, D. Gardes, and M. F. Rivet, *Nucl. Phys. A* **189**, 193 (1972).
- [8] T. Inamura, M. Ishihara, T. Fukuda, T. Shimoda, and K. Hiruta, *Phys. Lett.* **68B**, 51 (1977); *Foundations of Quantum Mechanics and Ordered Linear Spaces*, Lecture Notes in Physics Vol. 29 (Springer-Verlag, Berlin, 1974), p. 476.
- [9] D. J. Parker, J. Asher, T. W. Conlon, and I. Naqib, *Phys. Rev. C* **30**, 143 (1984).
- [10] D. J. Parker, J. J. Hogan, and J. Asher, *Phys. Rev. C* **31**, 477 (1985).
- [11] D. J. Parker, J. J. Hogan, and J. Asher, *Phys. Rev. C* **35**, 161 (1987).
- [12] D. J. Parker, J. J. Hogan, and J. Asher, *Z. Phys. A* **336**, 411 (1990).
- [13] J. J. Hogan, D. J. Parker, and J. Asher, *Z. Phys. A* **338**, 325 (1991).
- [14] A. Wolf, J. Todd, J. J. Hogan, and D. J. Parker (unpublished).
- [15] E. Gadioli, E. Gadioli-Erba, D. J. Parker, and J. Asher, *Phys. Rev. C* **32**, 1214 (1985).
- [16] E. Gadioli, E. Gadioli-Erba, J. J. Hogan, and B. V. Jacak, *Phys. Rev. C* **29**, 76 (1984).
- [17] J. Wilczynski, K. Siwek-Wilczynska, J. van Driel, S.

- Gonggrijp, D. C. J. M. Hageman, R. V. F. Janssens, J. Lukusiak, and R. H. Siemssen, *Phys. Rev. Lett.* **45**, 606 (1980).
- [18] K. Siwek-Wilczynka, E. H. du Marchie van Voorthuysen, J. van Popta, R. H. Siemssen, and J. Wilczynski, *Nucl. Phys.* **A330**, 150 (1979).
- [19] I. Tserruya, V. Steiner, Z. Fraenkel, P. Jacobs, D. G. Kovar, W. Henning, M. F. Vineyard, and B. G. Glagola, *Phys. Rev. Lett.* **60**, 14 (1988).
- [20] V. E. Viola, B. Back, K. L. Wolf, T. C. Awes, C. K. Gelbke, and H. Breuer, *Phys. Rev. C* **26**, 178 (1982).
- [21] T. Sikkeland, E. Haines, and V. E. Viola, *Phys. Rev.* **125**, 1350 (1962).
- [22] J. A. B. Goodall, UKAEA Report No. AERE-M3185, 1982.
- [23] U. Reus, W. Westmeier, and I. Warnecke, *At. Data Nucl. Data Tables* **29**, 1 (1983).
- [24] *Table of Isotopes*, edited by C. M. Lederer and V. S. Shirley (Wiley, New York, 1978).
- [25] L. C. Northcliffe and R. F. Schilling, *Nucl. Data Tables A* **7**, 233 (1970).
- [26] I. Dostrovsky, Z. Fraenkel, and G. Friedlander, *Phys. Rev.* **116**, 683 (1959).
- [27] A. H. Wapstra and G. Audi, *Nucl. Phys.* **A432**, 1 (1985).
- [28] P. E. Nemirowski and Yu. V. Adamchuck, *Nucl. Phys.* **39**, 551 (1962).
- [29] E. Fabrici, E. Gadioli, E. Gadioli-Erba, M. Galmarini, R. Fabbri, and G. Reffo, *Phys. Rev. C* **40**, 2548 (1989).
- [30] E. Gadioli, E. Gadioli-Erba, and J. J. Hogan, *Phys. Rev. C* **16**, 1404 (1977).
- [31] R. Serber, *Phys. Rev.* **72**, 1008 (1947).
- [32] N. Matsuoka, A. Shimizu, K. Hosono, T. Saito, M. Kondo, H. Sakaguchi, Y. Toba, A. Goto, F. Ohtani, and N. Nakanishi, *Nucl. Phys.* **A311**, 173 (1978).
- [33] M. Korolija, N. Cindro, and R. Caplar, *Phys. Rev. Lett.* **60**, 193 (1988).
- [34] E. Fabrici, E. Gadioli, and E. Gadioli-Erba, *Phys. Rev. C* **40**, 459 (1989).
- [35] T. D. Thomas, *Phys. Rev.* **116**, 703 (1959).